ENVIRONMENTAL ENGINEERING SCIENCE
Volume 37, Number 1, 2020
Mary Ann Liebert, Inc.
DOI: 10.1089/ees.2019.0146

Impacts of Varying Dam Outflow Elevations on Water Temperature, Dissolved Oxygen, and Nutrient Distributions in a Large Prairie Reservoir

Meghan K. Carr,[1] Amir Sadeghian,[1] Karl-Erich Lindenschmidt,[1,*] Karsten Rinke,[2] and Luis Morales-Marin[1]

[1]*Global Institute for Water Security, University of Saskatchewan, Saskatoon, Canada.*
[2]*Department of Lake Research, Helmholtz Centre for Environmental Research (UFZ), Magdeburg, Germany.*

Received: April 9, 2019 *Accepted in revised form: September 20, 2019*

Abstract

Dam operations are known to have significant impacts on reservoir hydrodynamics and solute transport processes. The Gardiner Dam, one of the structures that forms the Lake Diefenbaker reservoir located in the Canadian Prairies, is managed for hydropower generation and agricultural irrigation and is known to have widely altering temperature regimes and nutrient circulations. This study applies the hydrodynamic and nutrient CE-QUAL-W2 model to explore how various withdrawal depths (5, 15, 25, 35, 45, and 55 m) influence the concentrations and distribution of nutrients, temperature, and dissolved oxygen (DO) within the Lake Diefenbaker reservoir. As expected, the highest dissolved nutrient (phosphate, PO_4^{3-}-P and nitrate, NO_3^--N) concentrations were associated with hypoxic depth horizons in both studied years. During summer high flow period spillway operations impact the distribution of nutrients, water temperatures, and DO as increased epilimnion flow velocities route the incoming water through the surface of the reservoir and reduce mixing and surface warming. This reduces reservoir concentrations but can lead to increased outflow nitrogen (N) and phosphorus (P) concentrations. Lower withdrawal elevations pull warmer surface water deeper within the reservoir and decrease reservoir DO during summer stratification. During fall turnover low outflow elevations increase water column mixing and draws warmer water deeper, leading to slightly higher temperatures and nutrient concentrations than shallow withdrawal elevations. The 15 m depth (540 m above sea level) outflow generally provided the best compromise for overall reservoir and outflow nutrient reduction.

Keywords: dam withdrawal; dissolved oxygen; nutrients; reservoir; temperature; water quality

Introduction

Hydropower dams are typically built to produce electricity, and in some cases, they can serve as flood protection and provide water for irrigation and municipal needs. In addition, reservoirs may provide recreational activity opportunities. Despite these benefits, reservoir operation changes thermal regimes and nutrient transport affecting the biogeochemical cycling and the movement and fitness of biota (McKinley *et al.*, 1998; Fjeldstad *et al.*, 2012; Huang and Wang, 2018).

Some studies have examined the impacts of selective withdrawal on in-reservoir hydrodynamics and thermal structure (Gelda and Steven, 2007; Rheinheimer *et al.*, 2014; Weber *et al.*, 2017; Zheng *et al.*, 2017). Using a three-dimensional hydrodynamic model, Çalişkan and Elçi (2009) simulated the effects of selective water withdrawal on the hydrodynamics of the Tahtali reservoir, Turkey. They found that water withdrawal at the bottom outlet was the most effective choice to reduce anoxia by triggering mixing throughout the water column. Similarly, Casamitjana *et al.* (2003) analyzed the effects of water withdrawal scenarios on the thermal structure in the Boadella Reservoir, Spain, using a one-dimensional hydrodynamic model. They found that the thermocline location within the thermal structure coincides with the depth of the outlet.

Ma *et al.* (2008) used a two-dimensional (2D) hydrodynamic model to investigate changes of the thermal structure of underwater withdrawal scenarios in the Kouris Dam reservoir, Cyprus. They found that deep-water withdrawals enhance water column mixing by deepening the epilimnion and that the withdrawal scenarios can be implemented to manage water quality strategies. Although water withdrawal affects reservoir hydrodynamics and thermal structure, very little has

**Corresponding author:* Global Institute for Water Security, University of Saskatchewan, 11 Innovation Boulevard, Saskatoon S7N 3H5, Canada. *Phone:* (306)966-6174; *Fax:* (306)966-1193; *E-mail:* karl-erich.lindenschmidt@usask.ca

been investigated on the effects of in-reservoir dissolved oxygen (DO) and the transport and distribution of nutrients.

In this study, we focus on Lake Diefenbaker, a large multipurpose reservoir located in the Canadian Prairies that has been in operation since 1968 after the Gardiner Dam, one of the structures that forms Lake Diefenbaker, was built. As expected with the building of Gardiner Dam, the upstream reach shifted from fluvial to a combination of lacustrine and fluvial environments and the pattern and rates of sediment deposition, resuspension, bluff erosion, and shoreline retreat were significantly changed in the reservoir (Ashmore and Day, 1988; Sadeghian *et al.*, 2017). The draw-down reach, the section where conditions change from river to reservoir characteristics, generally has a bed elevation ranging between 556.87 meters above sea level (masl) maximum and 545.59 masl minimum water levels and therefore deposition in this reach affects the live storage capacity (Sadeghian *et al.*, 2017). In the reservoir section, the bed elevations are below the minimum operating water level and therefore affect dead storage capacity (Sadeghian *et al.*, 2017).

The reservoir acts as a significant phosphorus (P) sink, retaining 91% of external total phosphorus (TP) and 41% of dissolved reactive phosphorus (North *et al.*, 2015; Morales-Marín *et al.*, 2017). Lake Diefenbaker is thermally stratified, mixing once in the spring and once in the fall with a period of summer stratification (Phillips *et al.*, 2015). When the hypolimnion is isolated from the atmosphere during summer stratification, the bottom waters can become hypoxic resulting in significant Fe-associated P release (Doig *et al.*, 2017) and this internal loading can affect water quality of reservoirs (Nürnberg, 2009). Despite known P release from Diefenbaker sediments year round (North *et al.*, 2015; Doig *et al.*, 2017), it is not considered a significant source of P to the reservoir in stratified regions such as at the dam outflow (North *et al.*, 2015). Although these studies provide insight into impacts because of the creation of the reservoir, little is known about the impacts of current dam operations on the chemical and nutrient characteristics of Lake Diefenbaker.

Separating dam-related impacts from other anthropogenic sources such as urbanization and agriculture and sufficient high-quality data collection to increase statistical power remain as shortcomings of models that seek to predict dam-related ecosystem shifts (Nguyen *et al.*, 2018). Accordingly, models remain a valuable tool for investigating dam impacts on both reservoir and downstream water quality and temperature (Park *et al.*, 2014; Zouabi-Aloui *et al.*, 2015; Saadatpour *et al.*, 2017). In this research study, the 2D hydrodynamic water quality CE-QUAL-W2 (Cole and Wells, 2008) model has been implemented to provide insights on the impacts of various withdrawal elevations on the in-reservoir nutrient and water chemistry characteristics of Lake Diefenbaker. The effects on the downstream water bodies and ecosystems (McKinley *et al.*, 1998; Fjeldstad *et al.*, 2012; Huang and Wang, 2018), because of changes in the temperature, DO, and nutrient concentration of the released water, are analyzed in the Discussion section.

Methods

Study area

Lake Diefenbaker is a large multipurpose reservoir located in the Canadian Prairies (Fig. 1) that went into operation in 1967 to produce hydropower (1,000 GWh annually). The reservoir was formed after the construction of Gardiner and Qu'Appelle dams located on the left and right arms of the reservoir, respectively. The reservoir is 225 km long and has a surface area of 394 km^2, allowing 9.8 km^3 of water to be stored. The reservoir is located along the South Saskatchewan River (SSR), with 95% of the reservoir inflows coming from the SSR and 5% from Swift Current Creek and other small tributaries. The reservoir not only regulates the SSR streamflows, but is also a sink for sediment and nutrients exported and transported from the SSR catchment.

The reservoir also provides water for agricultural irrigation and domestic and industrial uses, and significant downstream flood protection. Since its construction, the reservoir has also been used for aquaculture and recreational activities, and serves as habitat for many aquatic animals and birds (WSA, 2012). This study focuses on the entire length of Lake Diefenbaker extending from the upstream model boundary conditions downstream to the Gardiner Dam (Fig. 1).

Model description

Based on the complex geometry of the reservoir, duration of the desired study period, and the level of details required for the study, we chose CE-QUAl-W2 (Cole and Hannan, 1990) version 4.0 as a suitable model for this reservoir. The CE-QUAL-W2 model is a laterally averaged water quality model developed by the Environmental Protection Agency for comprehensive 2D water quality studies (Cole and Wells, 2008). The model solves momentum and transport equations in Cartesian coordinates, and supports variable horizontal segmentation and vertical layering. Input data including meteorological data (air temperature, dew point temperature, wind speed and direction, precipitation, solar radiation, and cloud cover), flow (inflow, outflow, and nonpoint source flows), water temperature, algae, nutrient (carbon, nitrogen, and phosphorous component), and water quality variables (DO, pH, and alkalinity) can be imported to the model at any temporal resolution. The model has a long (>40 years) development history with many applications all over the world including Canada (Sadeghian *et al.*, 2015; Saadatpour *et al.*, 2017).

CE-QUAL-W2 setup for this study was taken from an earlier study performed on Lake Diefenbaker (Sadeghian *et al.*, 2015, 2018). The reservoir basin is discretized in 87 horizontal segments starting at Saskatchewan highway 4 at the upstream extending to the downstream Gardiner Dam and the Qu'Appelle Dam, and 1-m vertical layers with a maximum of 60 layers at the deepest point near the Gardiner Dam. Each segment of the reservoir model was also characterized by its horizontal orientation and bottom friction.

Model calibration

A Monte-Carlo analysis with 1,000 simulations was performed to evaluate model sensitivity to different parameters, followed by automatic optimization for model calibration. Calibration of the water temperature model was performed by minimizing the sum of squared error and the root mean square error (RMSE) based on simulated time series and observed profiles taken at 16 locations across the reservoir (Sadeghian *et al.*, 2015). Acceptable model performance was obtained with RMSE <2°C with optimum values of 0.85 and

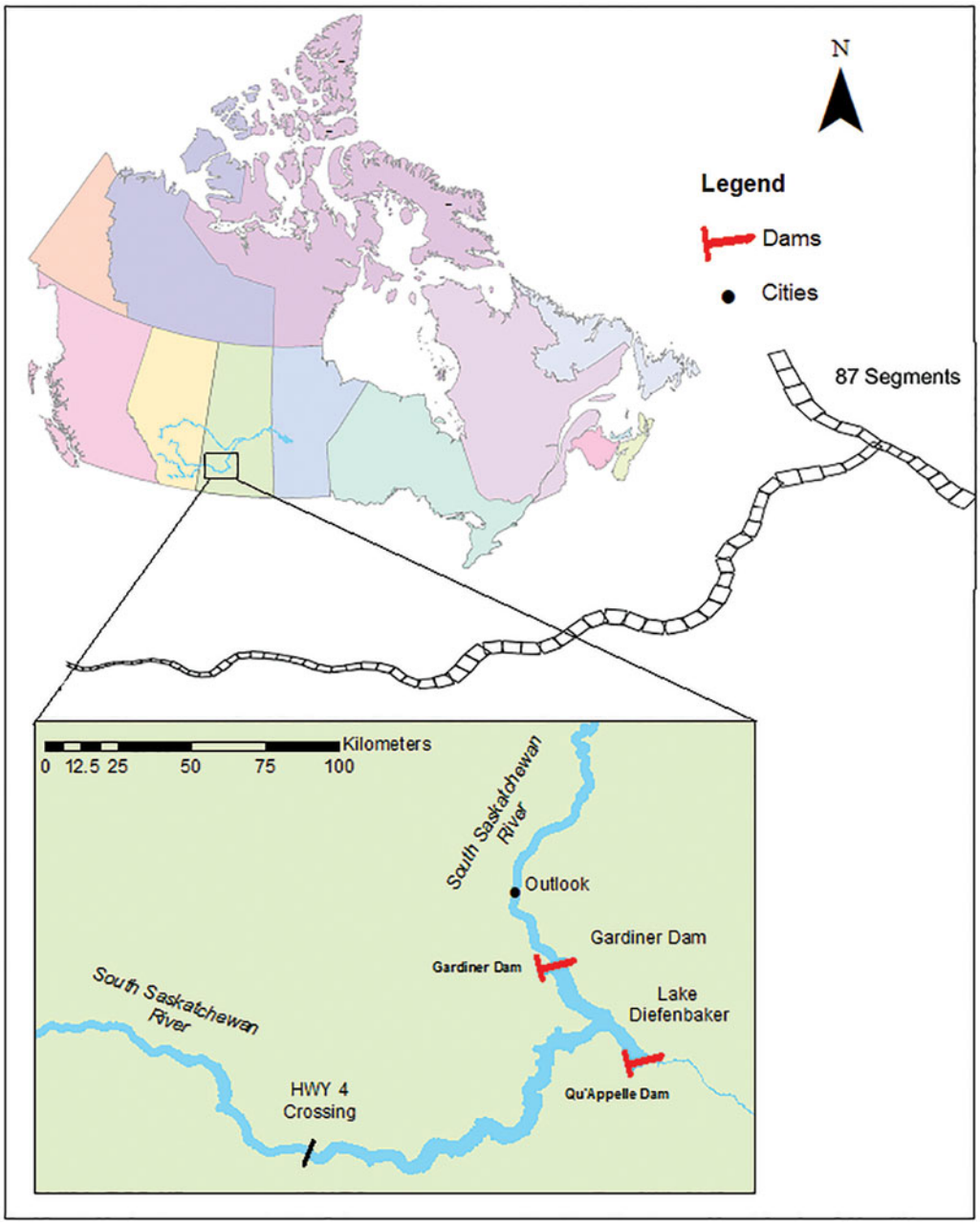

FIG. 1. Lake Diefenbaker Reservoir enclosed by the Gardiner and Qu'Appelle Dams. The inflowing South Saskatchewan River and outflowing Lower South Saskatchewan and Qu'Appelle Rivers are included. The CE-QUAL-W2 model boundaries run from the upstream boundary shown in the map down to and including the reach closed by the Qu'Appelle and Gardiner dams.

0.80 for wind sheltering coefficient and solar radiation shading coefficient, respectively.

In contrast to the calibration of the water temperature, for which a Monte-Carlo approach was implemented, the calibration of the water quality model was performed manually because of the extensive computational time. Sadeghian *et al.* (2018) calibrated the model for particulate organic carbon (POC), particulate organic nitrogen (PON), total nitrogen (TN), TP, total dissolved solids, phosphate (PO_4^{3-}-P), organic P, ammonium (NH_4^+), nitrate (NO_3^--N), organic N, and DO. Model parameters affecting chemical and biological reactions in the system such as algal rates (growth, respiration, excretion, mortality, half-saturation for nutrients, and light saturation), algal temperature rates, algal stoichiometry, organic matter (dissolved and particulate) decay and settling rates, inorganic phosphorus sediment release rate and partitioning coefficient for suspended solids, ammonium decay rate and sediment release rate, nitrate decay rate and denitrification rate from sediments, and sediment oxygen demand were adjusted manually in the model. Model performance was evaluated based on the averaged root mean squared error (RMSEav), which is equivalent to RMSE divided by the

average of observed values. Values of RMSEav equal to 0.17, 0.66, 0.69, 0.38, and 0.67 were obtained for DO, POC, PON, TN, and TP, respectively (Sadeghian *et al.*, 2018).

Because of the small amount of reservoir main inlet and in-reservoir observations, the authors found that much smaller simulation errors are obtained when water samples are collected over more places and with higher frequencies, at least weekly/monthly time intervals, for chemistry analysis. Discrepancies were more pronounced, especially, for variables such as PO_4^{3-}-P and total suspended solids because of the little observation data available. According to North *et al.* (2015), ~84% of the phosphorous loading that flows into Lake Diefenbaker occurs during the high flow period that requires minimum weekly observation frequencies (Weagle and Crosley, 1989). A more detailed analysis of model calibration, model uncertainty, and parameter sensitivity is included in Sadeghian *et al.* (2015, 2018).

Modeling scenarios

Six water withdrawal scenarios starting at 5 m from the reservoir's bed with 10-m intervals up to 55 m from the bed (5, 15, 25, 35, 45, and 55 m depths which, respectively, correspond to the 550, 540, 530, 520, 510, and 500 masl [geodetic elevations]) were used. Model simulations were performed from 2011 to 2013, which included an extreme flood event during this period, so that increases in flood surges were investigated with regard to dam operations (Fig. A1 in Supplementary Appendix). These flood events were caused by heavy rainfall and runoff at lower elevations exacerbated by rain-on-snow runoff from high elevations because of late lying snow packs. These floodwaters were also characterized by higher than usual turbidity because of debris flows that resulted in the movement of large amounts of sediment in the headwaters (Pomeroy and Shook, 2012).

Animations of contour plots were used to analyze simulated water temperature, DO, and nutrient concentration changes through 2011 and 2013. Specifically, we analyzed the following model output variables: water temperature, DO, TP, orthophosphate as P (PO_4^{3-}-P), a proxy for soluble, labile P, TN, nitrate as nitrogen (NO_3^--N), a proxy for soluble, labile N, and ammonium (NH_4^+-N). Flow velocity vectors, which are represented by the longitudinal (v_x) and the vertical (v_z) components, were used to infer how flow particles move through the reservoir and how hydrodynamics may impact the distribution and concentration of the studied variables. Changes were specifically investigated for the spring turnover (from April 15 to May 31) (Supplementary Appendix), summer stratification (from June 1 to August 31), and fall turnover (from September 15 to October 31) periods of 2011 and 2013 to give a broad understanding of seasonal change and outflow elevation impacts on nutrient concentrations and distributions. Spillway versus turbine outflow (Fig. A1 in Supplementary Appendix), which had a considerable impact during the 2013 flooding event, was also considered in interpreting model outputs.

Results

Summer stratification

During summer there was a period of flooding in 2011 that occurred ~1 month earlier than in 2013, before the lake was strongly stratified. In 2011, total nutrient concentration peaks occurred in the first half of June when the floodwaters entered the lake, although highest dissolved nutrient and lowest DO concentrations lagged a month behind. The 2013 peak influx of floodwaters entered the lake later than 2011 and an associated large increase in total nutrient aligned with the late June/early July peak of discharge. Similar to 2011, an associated increase in dissolved nutrients and decrease in DO lagged behind total nutrients, occurring end of July when high total nutrient (and likely suspended solids) concentrations were concentrated along the bottom, increasing DO demand when the lake was strongly stratified. The 2013 total nutrient concentrations and DO lows were greater than in 2011. Through June and July 2011, the surface became warmer and higher temperatures (Fig. 2) occurred at deeper layers for low withdrawal elevations in both 2011 and 2013. Despite this, outflow temperatures had ~10°C difference between 500 and 550 masl outflows in both years. Temperatures were higher and occurred at deeper layers in 2011 than 2013 and greater regions of low bottom temperatures were maintained in 2013.

In contrast to water temperature, June and July 2011 DO concentrations (Fig. 3) dropped considerably along the bottom of the reservoir, particularly for lower withdrawal elevations that released water with slightly lower DO concentration (generally ~1 mg/L lower). In contrast, the July 2013 lower withdrawal elevations typically released flow with higher DO concentrations (generally ~2 mg/L higher). In both years, lower withdrawal elevations caused greater areas of low DO to spread within the reservoir. Lower outflow elevations were associated with greater decreases in reservoir DO concentrations but higher outflow concentrations (~2 mg/L higher). In contrast to spring turnover (Fig. A3 in Supplementary Appendix), shallower 540 and 550 masl elevations provided the best balance of reservoir and outflow DO concentrations in both 2011 and 2013 (Fig. 3). Through June 2011, the lowest DO (Fig. A9 in Supplementary Appendix), and most of the highest TP (Fig. A10 in Supplementary Appendix) concentrations, moved across the epilimnion in the region with the highest flows. In both 2011 and 2013, a greater proportion of flow was diverted through the spillway. Through July, surface velocities decreased substantially as spillway diversions decreased and high TP (Fig. 4) and water with low DO concentrations began to move along the bottom of the reservoir rather than be routed along the surface.

In July 2011, after the high flow peak in June, higher TP (Fig. 4) concentrations were distributed more at lower withdrawal elevations although all outflows remained the same. PO_4^{3-}-P concentrations increased through mid-June (areas of 17–20 μg/L) moving along both the surface and the bottom of the reservoir for all scenarios. TP concentrations peaked by end of June when there was a large influx of high TP concentration (up to 70 μg/L) and 540–550 masl outflows increased to 20 μg/L, whereas the rest dropped to 10 μg/L. By mid-July, high concentrations (60–70 μg/L) decreased but 550 masl (5 m) outflows jumped to 40 μg/L, whereas deep withdrawals remained at 10 μg/L. Through July 2011, water with higher concentrations moved along the bottom of the reservoir and in 2013 water with higher concentrations moved along the top of the reservoir.

The 2013 streamflows had greater concentrations of both TP and PO_4^{3-}-P moving into the reservoir through July (Figs. 4 and 5). By mid-July, water surface concentrations

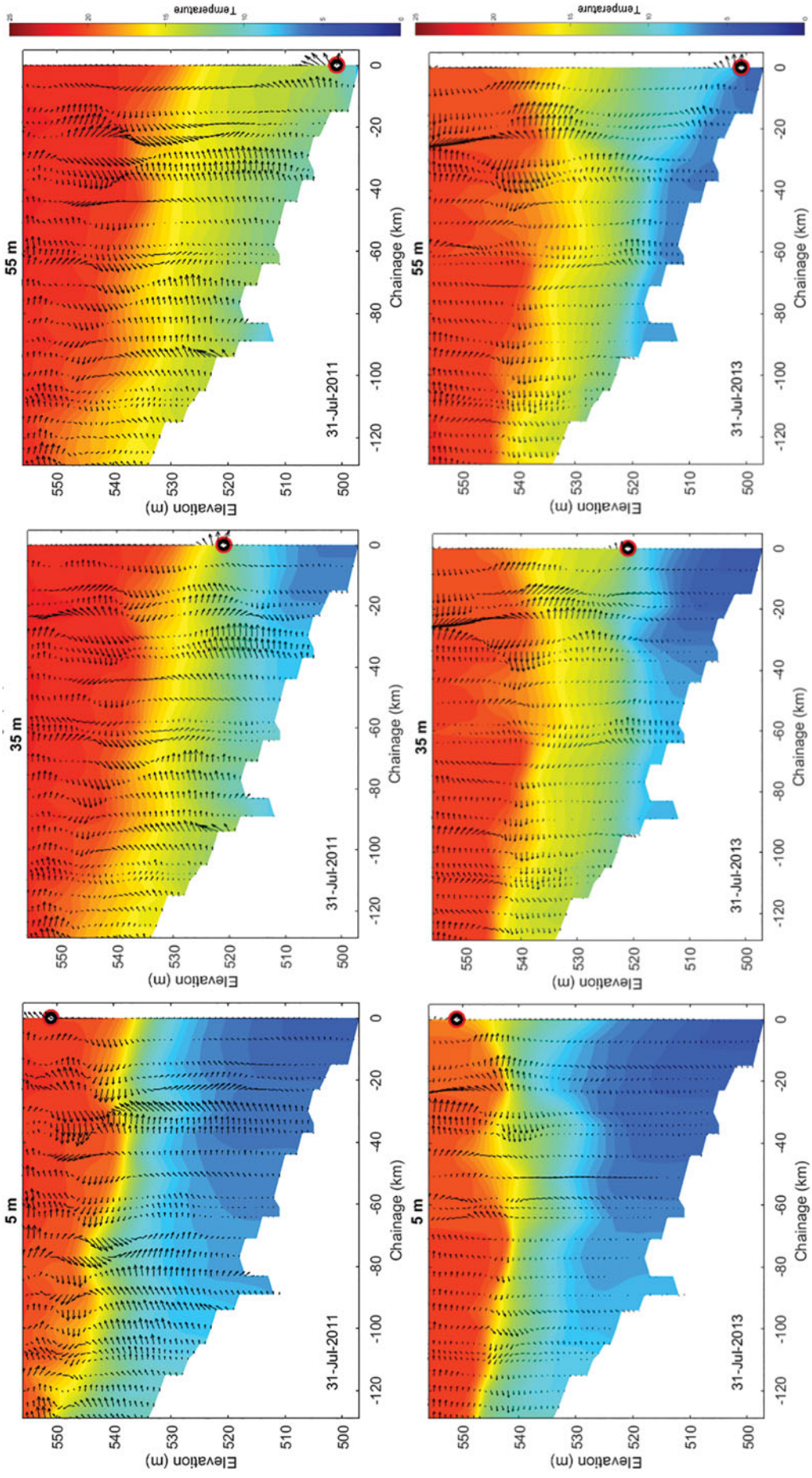

FIG. 2. July 31, 2011 and 2013 temperature profiles for 5, 35, and 55 m outflows.

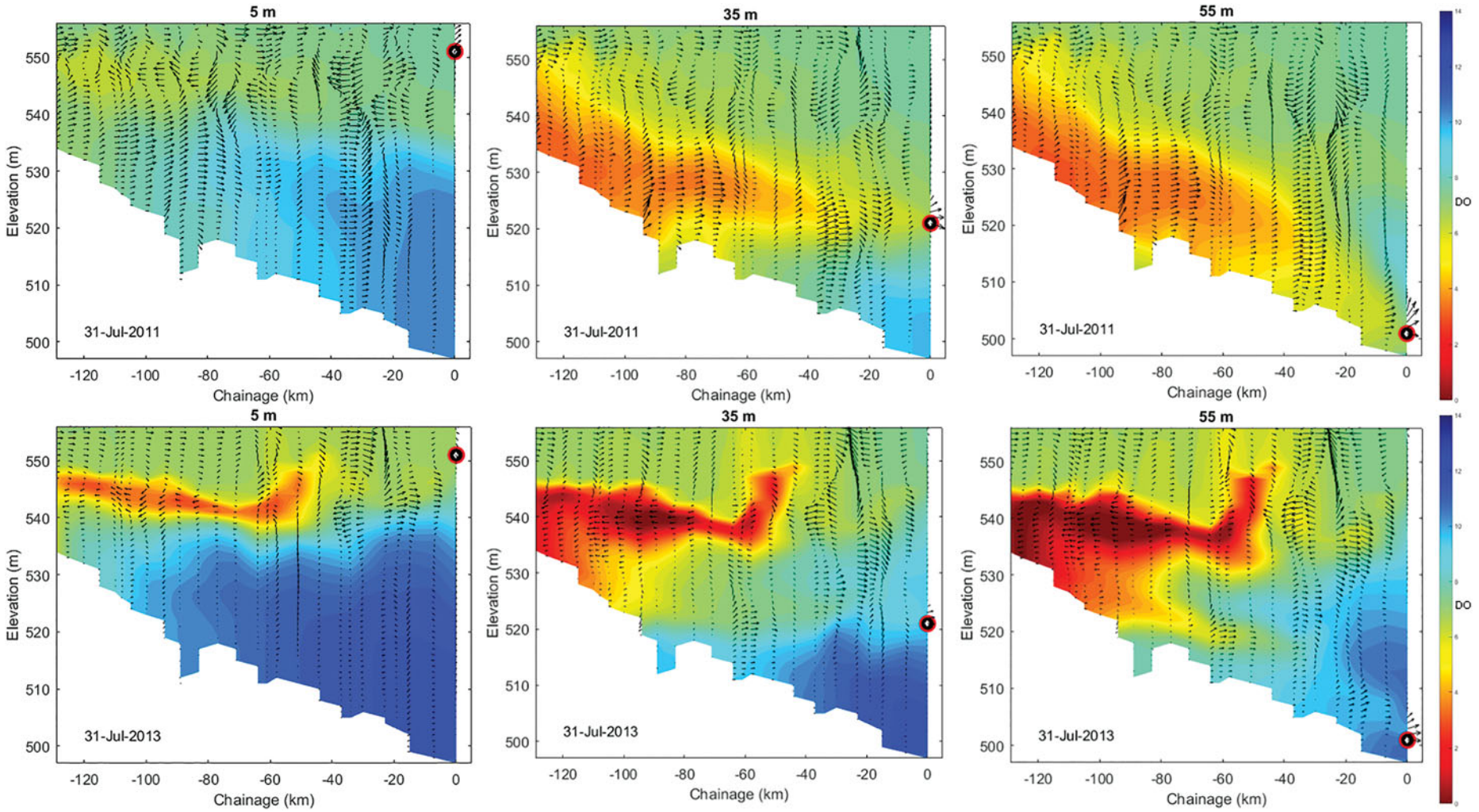

FIG. 3. July 31, 2011 and 2013 DO profiles for 5, 35, and 55 m outflows. DO, dissolved oxygen.

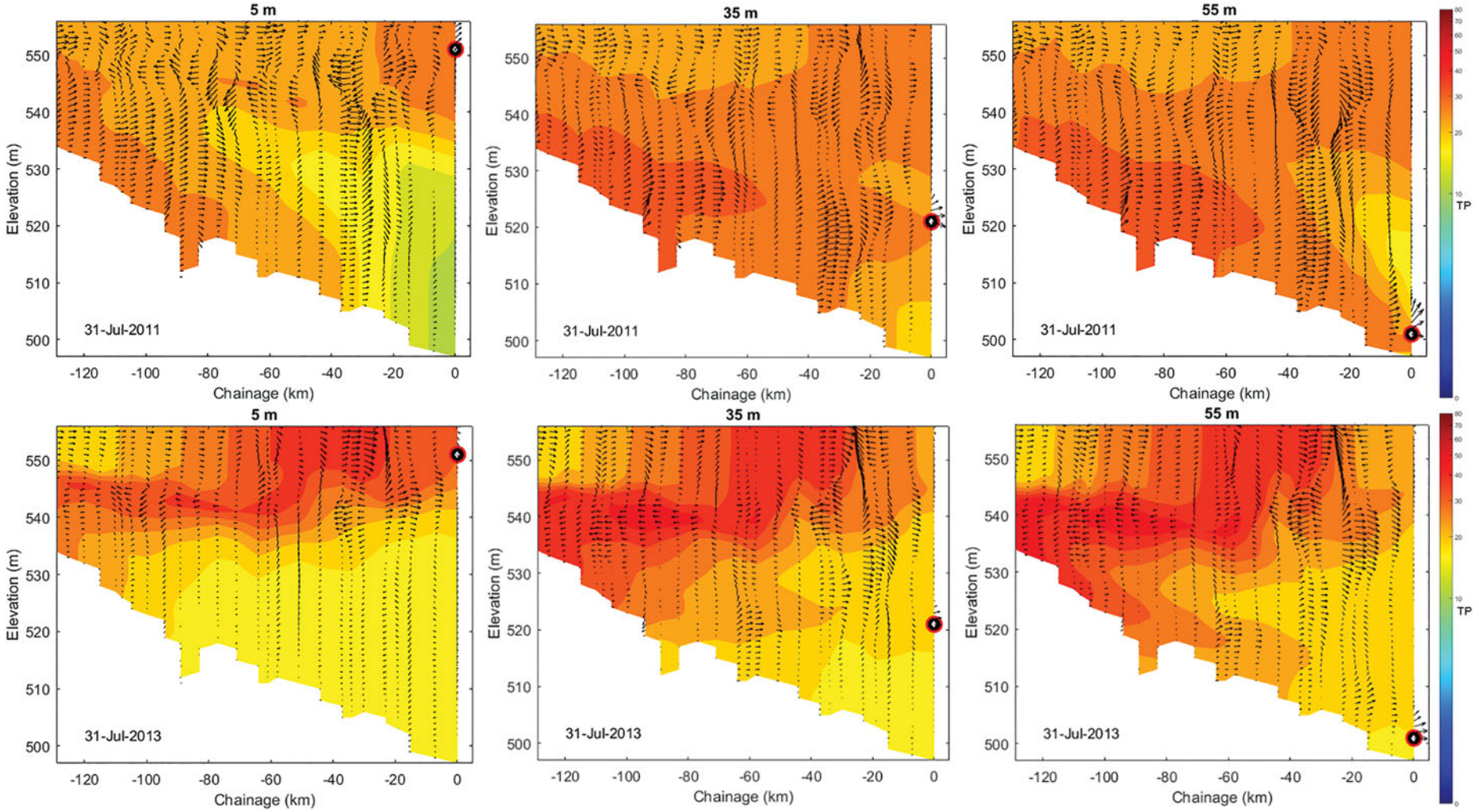

FIG. 4. July 31, 2011 and 2013 TP profiles for 5, 35, and 55 m outflows. TP, total phosphorus.

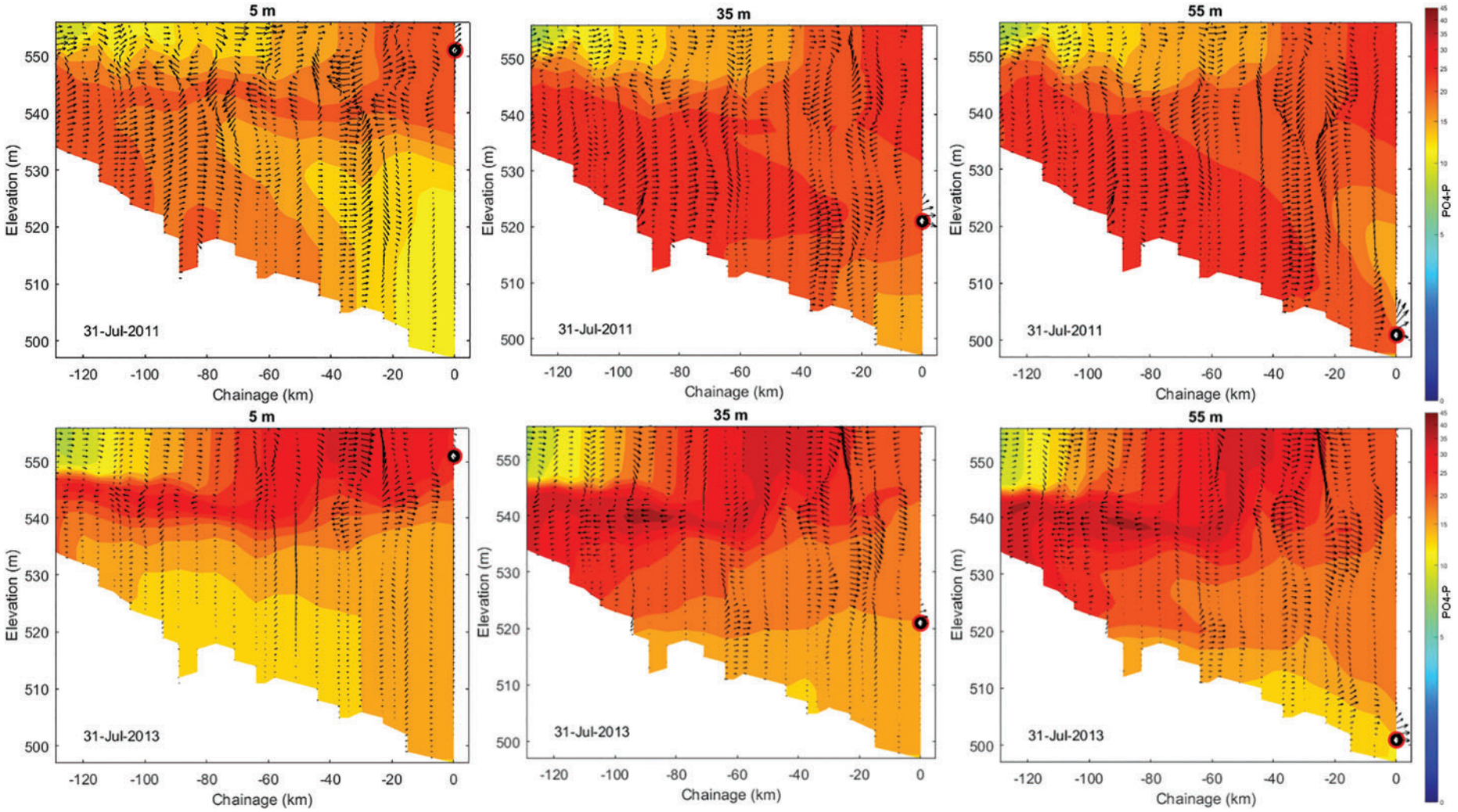

FIG. 5. July 31, 2011 and 2013 PO_4^{3-} – P profiles for 5, 35, and 55 m outflows.

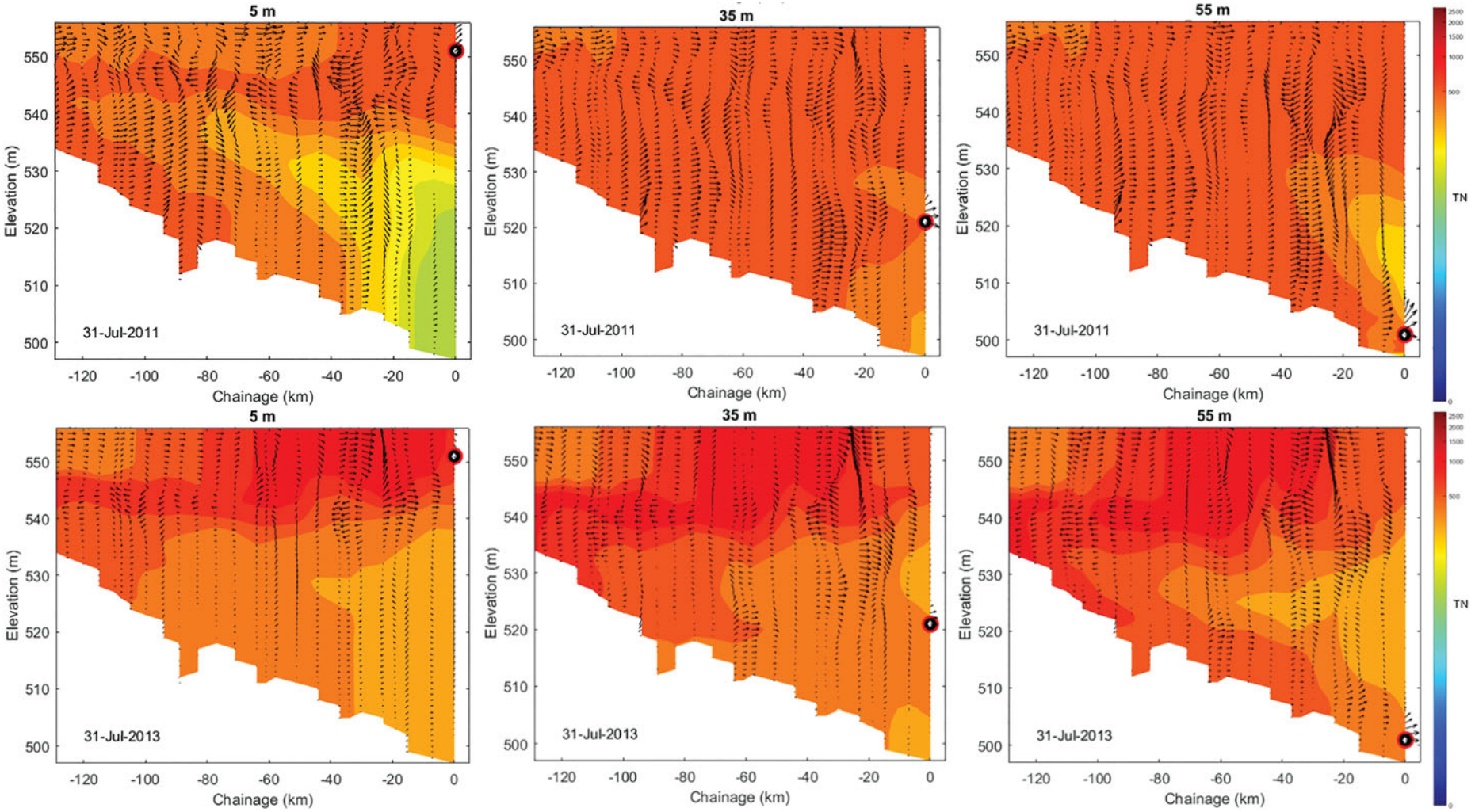

FIG. 6. July 31, 2011 and 2013 TN profiles for 5, 35, and 55 m outflows. TN, total nitrogen.

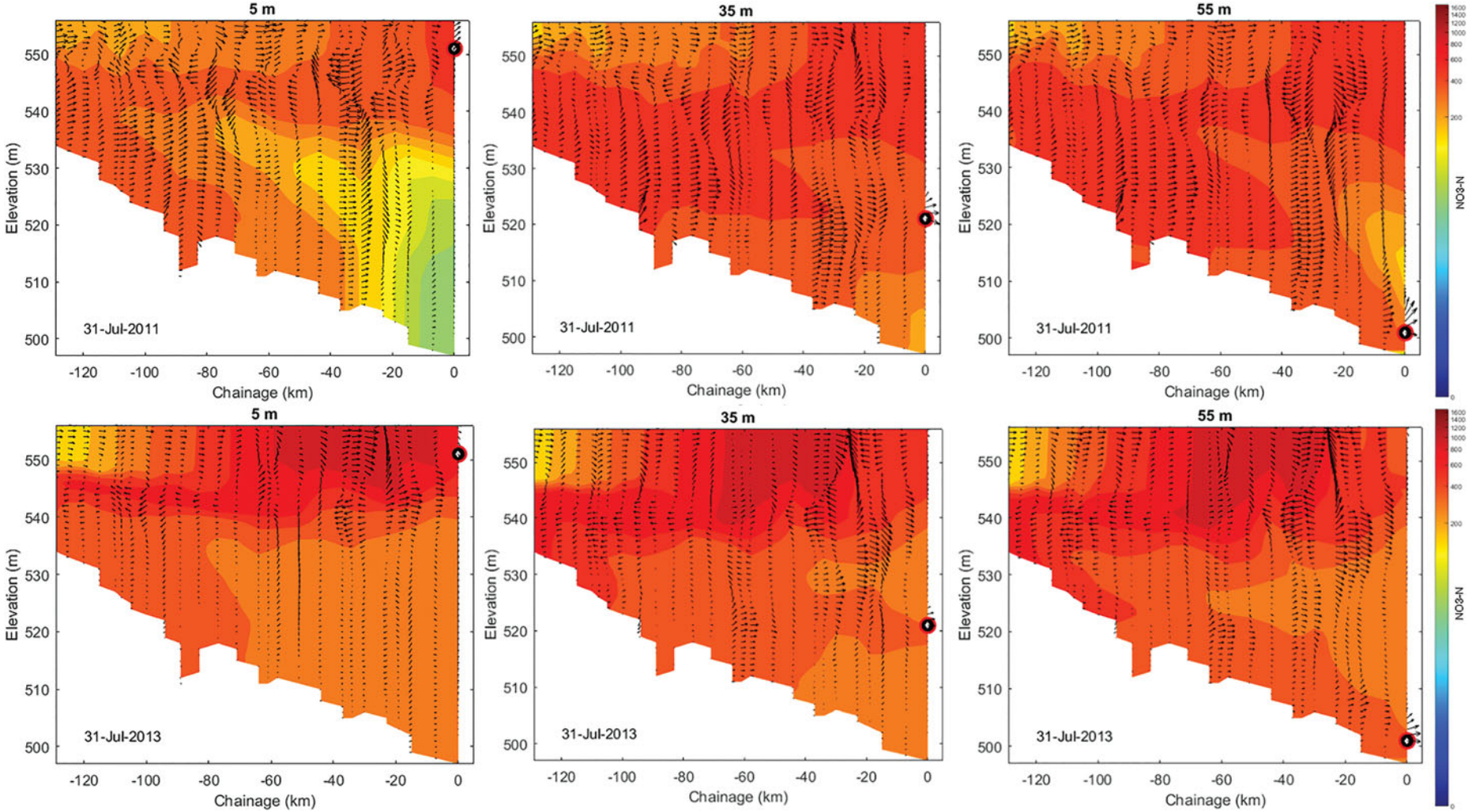

FIG. 7. July 31, 2011 and 2013 $NO_3^- - N$ profiles for 5, 35, and 55 m outflows.

increased substantially and higher elevations released flow with higher concentrations of PO_4^{3-}-P. Water with higher TP concentrations were further distributed throughout the reservoir through July with all outflow elevations reaching 20 μg/L. PO_4^{3-}-P concentrations peaked at the end of July and into August with lower elevations, releasing flow with higher concentrations in August (Fig. 10).

Similar to TP and PO_4^{3-}-P, in 2011, water with high TN (Fig. 6) and NO_3^--N (Fig. 7) concentrations were pulled deeper into the reservoir for low elevation outflows without changing outflow concentrations. However, in 2013, low elevations pull water with higher concentration deeper but outflow concentrations decrease for both TN and NO_3^--N. Streamflows with greater concentrations of both TN and NO_3^--N entered the reservoir in 2013. TN began to increase more rapidly (up to $\sim$1,500 μg/L) in the upstream portion of the reservoir than in 2011 with a massive peak in concentrations occurring at the end of June/start of July (up to $\sim$2,500 μg/L) and higher outflow elevations (540 and 550 masl) releasing flow with higher concentrations through July. NO_3^--N concentrations increased substantially through June and into July increasing 540 masl to 400 μg/L and 550 masl to 800 μg/L and the others remained at 200 μg/L. The 1,400 μg/L concentration water largely dissipated by mid-July. Concentrations peaked at 1,600 μg/L in very small upstream regions on July 3 and 4. By end of July, 1,400 and 1,200 μg/L concentration water were fully dissipated, 540 masl remained at 400 μg/L and 550 masl at 800 μg/L. Although different withdrawal scenarios seemed to have a greater impact in 2011 than 2013, deeper withdrawal elevations in 2013 resulted in lower outflow concentrations for both TN and NO_3^--N while having little impact on reservoir concentrations. In both years the majority of N was in soluble form and 520–540 masl outflows coincided with the best scenarios for P (Figs. 4 and 5) reduction with little change in N concentrations.

At the very end of June and into July of both years, a plug of high NH_4^+-N (Fig. 8) concentration water moved into the reservoir reaching values up to 40 μg/L in 2011 and 100 μg/L in 2013. Greater NH_4^+-N concentrations were observed in 2013 and, as with other variables, shallower withdrawal elevations tended to result in lower reservoir concentrations with little increase in outflow concentrations.

Hypoxic conditions

In 2011, a hypoxic layer was formed along the bottom in mid-August for lower withdrawal elevations. This layer peaked in size mid-September (Fig. 9) and lasted until beginning of October. In 2011, TN concentrations peaked mid-June near the surface, whereas NO_3^--N (Fig. 10) peaked at the start of June. Overall greater reservoir NO_3^--N concentrations occurred through mid-August, before the period of lowest DO. Regions of high PO_4^{3-}-P (Fig. 11) concentrations increased through July and August along the bottom in the hypoxic region.

In 2013, DO levels decreased more than in 2011 with anoxic regions beginning to form in the upper half of the water column mid-July for the 500–540 masl scenarios. The regions of anoxia increased through July and an anoxic region was also formed for the 550 masl scenario (which declined by July 28) (Fig. 12). Similar to 2011, the largest regions of low DO occurred through the end of August and beginning of September for the 500–520 masl scenarios (Fig. 13). The anoxic region was gone by August 31 for 540 masl, September 27 for 530 masl, October 2 for 520 masl, October 23 for 500 masl, and October 26 for 510 masl. In 2013, TN and NO_3^--N concentrations peaked near the surface at the end of June through the beginning of July, whereas overall reservoir NO_3^--N concentrations increased through July as anoxic regions grew. Regions of highest PO_4^{3-}-P (Fig. 14) concentrations coincided with July anoxic regions.

Advanced stratification

Through August, variable concentration patterns were similar to July. PO_4^{3-}-P and NO_3^--N concentrations were higher in 2013 than 2011 and outflows were more variable. Surface concentrations dropped since July and distribution patterns were very similar across all scenarios in both years. In 2013, NH_4^+-N concentrations decreased more slowly through August with all outflows reaching 5 μg/L by the end of the month. Overall the greatest spillway discharge during the study period occurred through the latter half of June 2013, during the summer stratification period. The greatest spillway discharge in 2011 also occurred through June during summer stratification although peak spillway discharge was considerably higher in 2013 (see central panel in Fig. A1 in Supplementary Appendix).

Discussion

Implications of water withdrawals in reservoir dynamics

Mid-elevation withdrawals (530 and 540 masl or 25 and 15 m, respectively) are the optimal withdrawal depths to balance reservoir and downstream temperature, DO, and nutrient concentrations. A comparison between years shows that 2011 had the highest outflow discharge proportion diverted to the spillway during spring turnover (Fig. A1 in Supplementary Appendix). In 2013, the year of greatest summer flooding, the surface spillway was only used for a short period in early May. This difference in the type of prevailing outflow may have influenced the distribution of variable concentrations within the reservoir. Power house/turbine-dominated outflows (below surface outflow) likely cause greater mixing in the water column near the dam by having a lower outflow elevation than the spillway. This pattern is apparent with DO, water temperature, and PO_4^{3-}-P.

Through June and July 2011, the surface warms further and water with higher temperatures (Fig. 2) moved deeper for low withdrawal elevations in both 2011 and 2013. Despite this, outflows have $\sim$10°C difference between 500 and 550 masl outflows in both years. Water temperatures were higher and occurred at deeper layers in 2011 than 2013 and greater regions of low bottom temperatures were maintained in 2013 (likely because of high June surface velocities reducing surface warming). In both 2011 and 2013, a greater proportion of flow was diverted through the spillway (Fig. A1 in Supplementary Appendix) that likely contributed to the increased flow velocities through the epilimnion in the latter half of June.

The 2013 total nutrient and DO concentration lows were greater than in 2011, likely because of the greater load of turbid water and associated labile fine sediment in that year (Pomeroy and Shook, 2012; Hudson and Vandergucht, 2015;

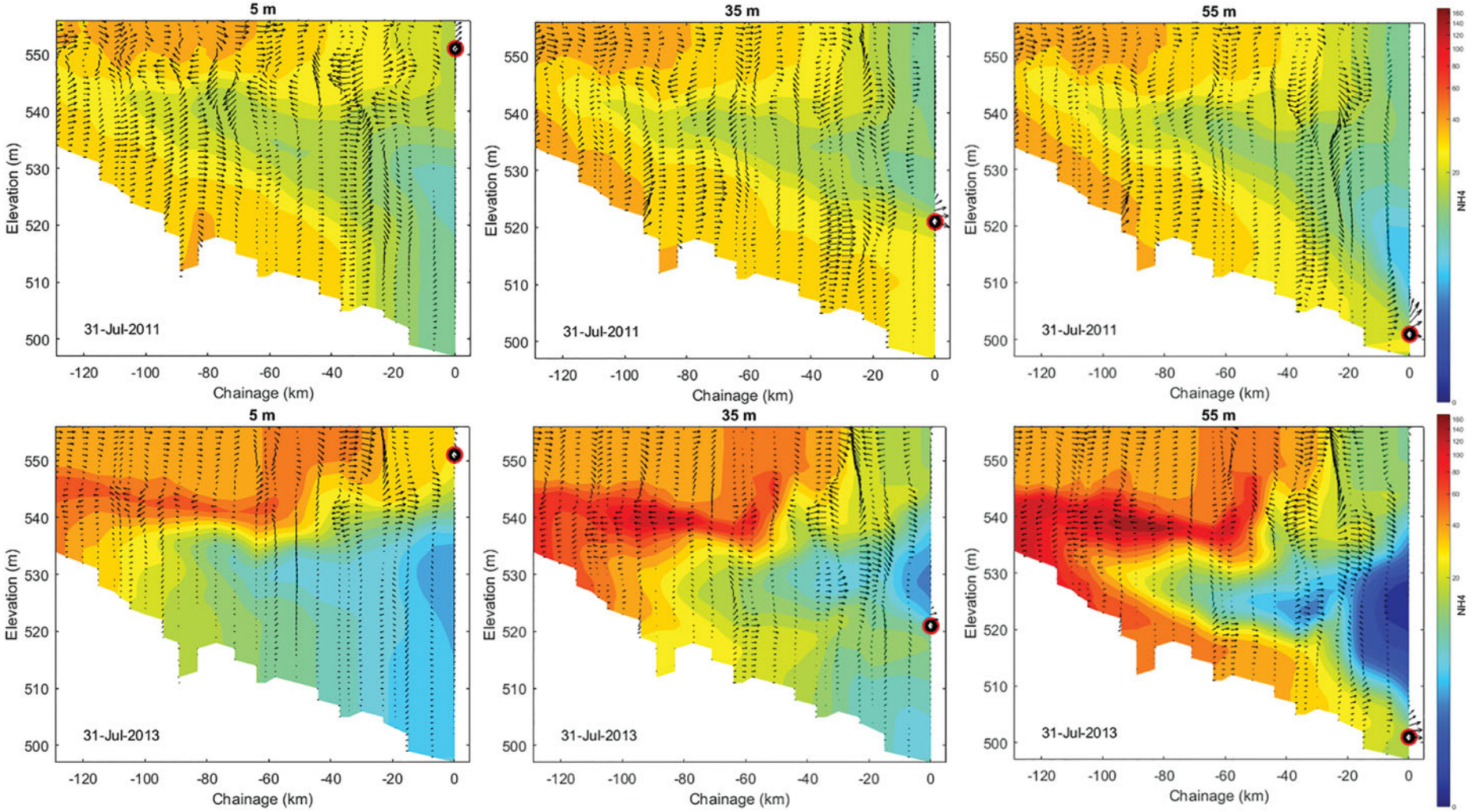

FIG. 8. July 31, 2011 and 2013 $NH_4^+ - N$ profiles for 5, 35, and 55 m outflows.

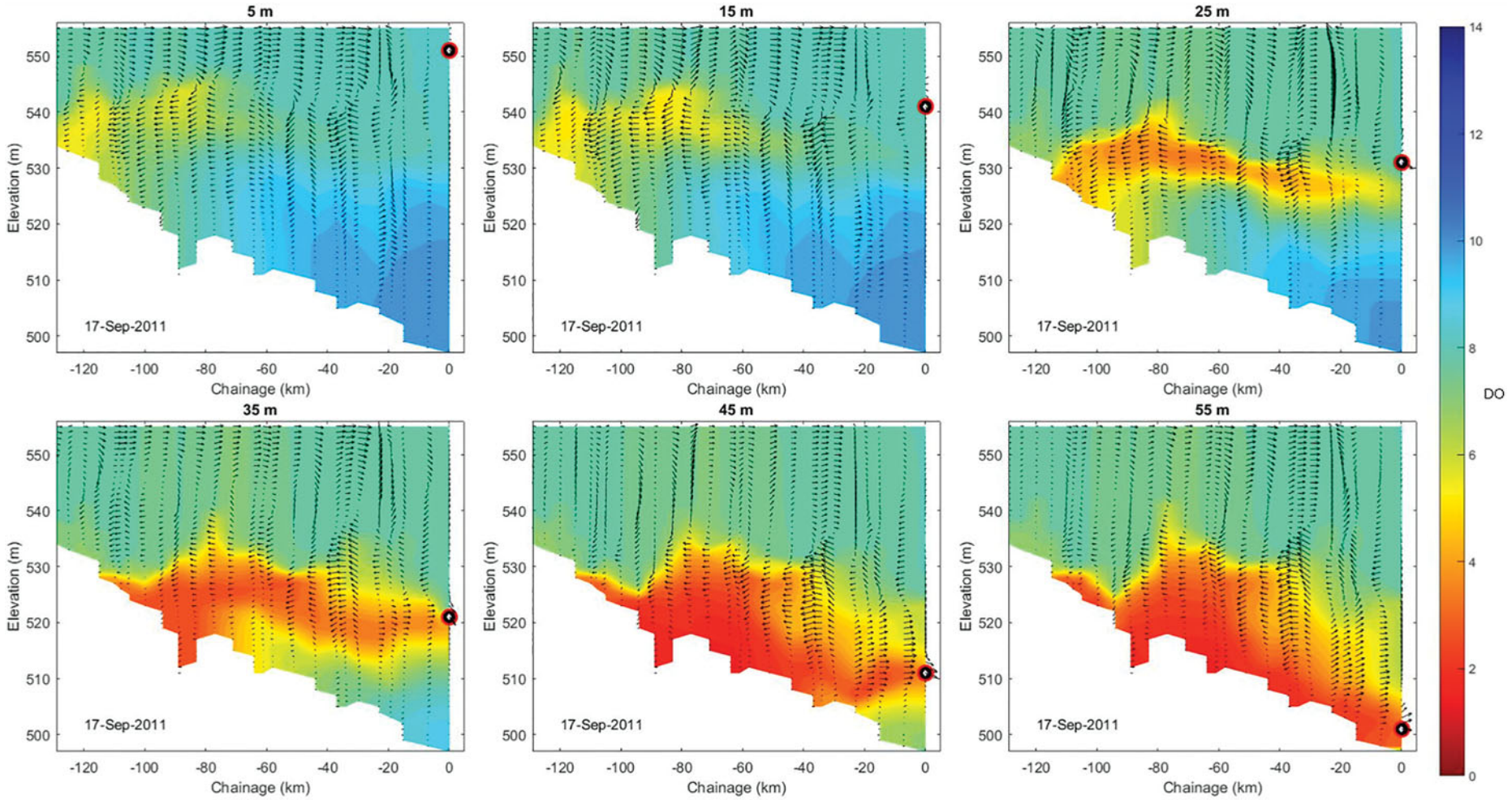

FIG. 9. September 17, 2011 DO profiles for 5, 35, and 55 m outflows during peak hypoxic conditions.

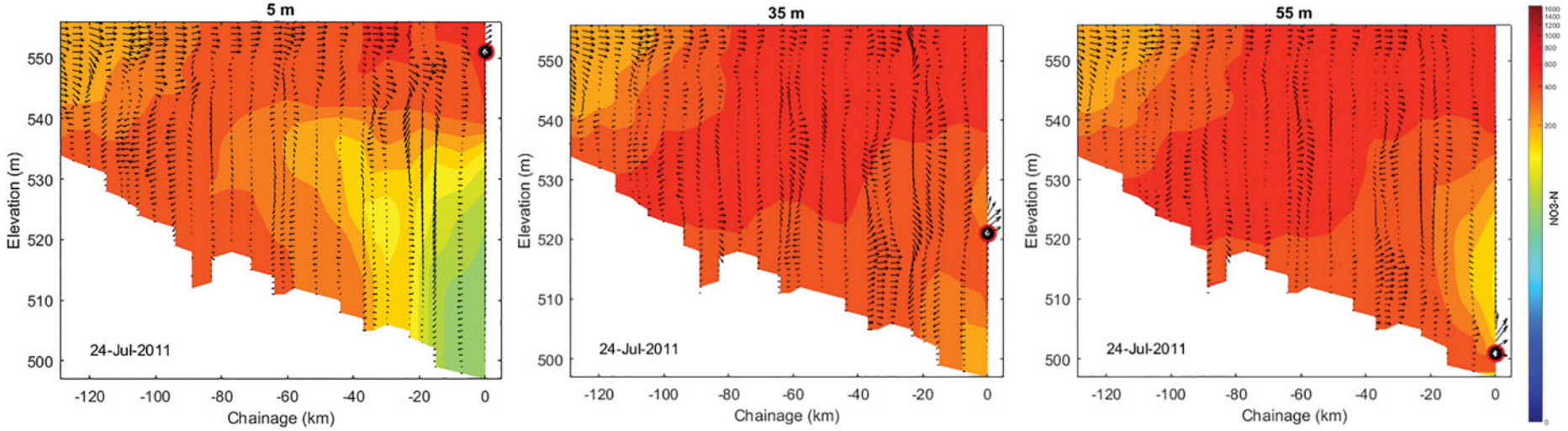

FIG. 10. July 24, 2011 NO_3^- – N profiles for 5, 35, and 55 m outflows during hypoxic conditions.

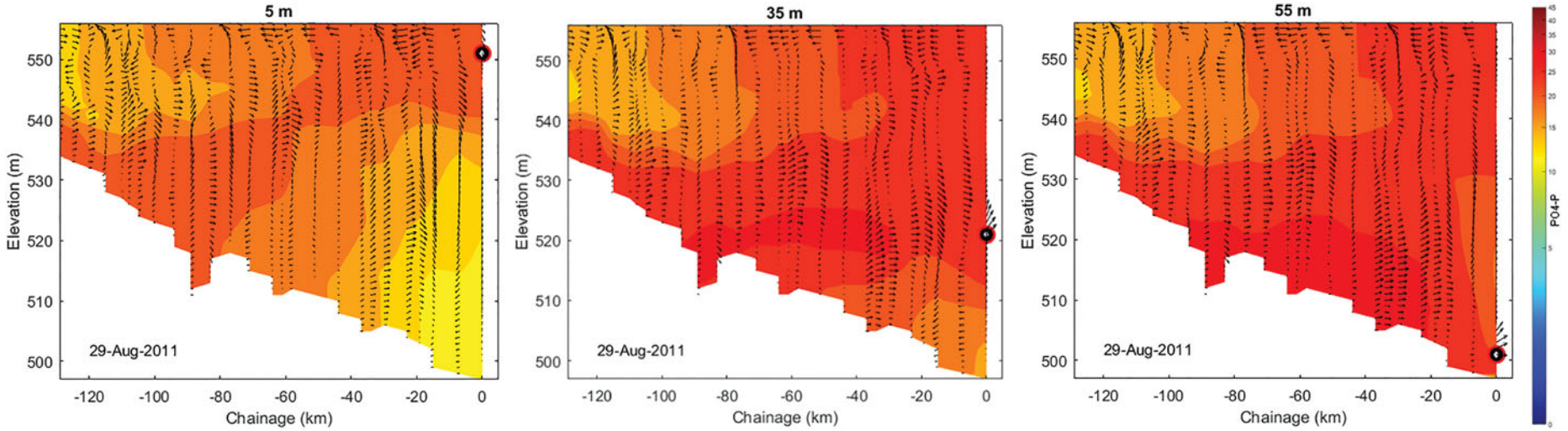

FIG. 11. August 29, 2011 PO_4^{3-} – P profiles for 5, 35, and 55 m outflows during hypoxic conditions.

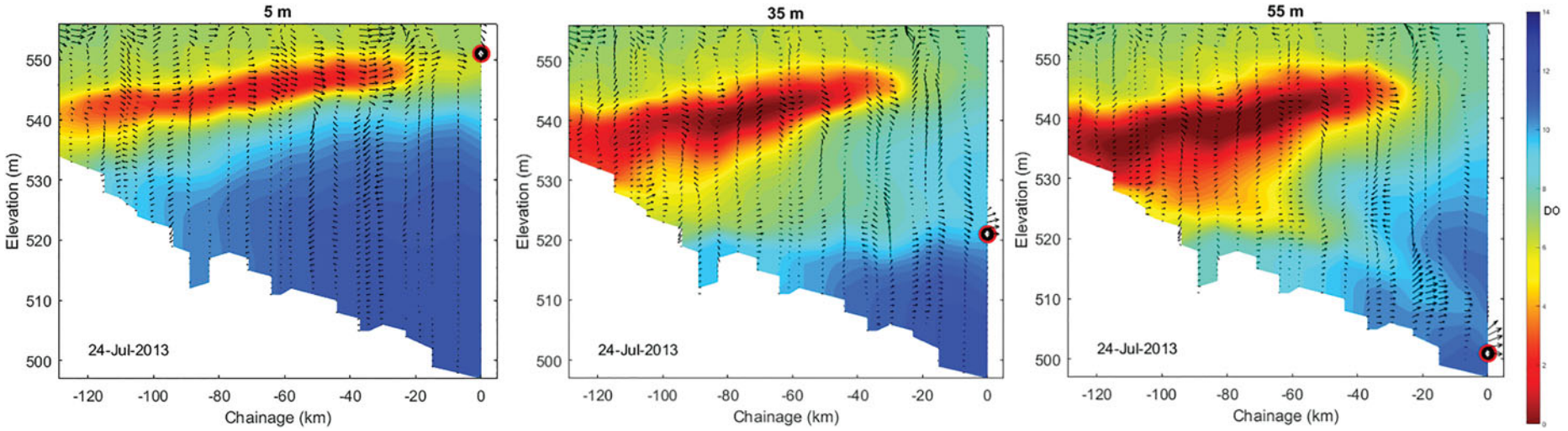

FIG. 12. July 24, 2013 DO profiles for 5, 35, and 55 m outflows during hypoxic conditions.

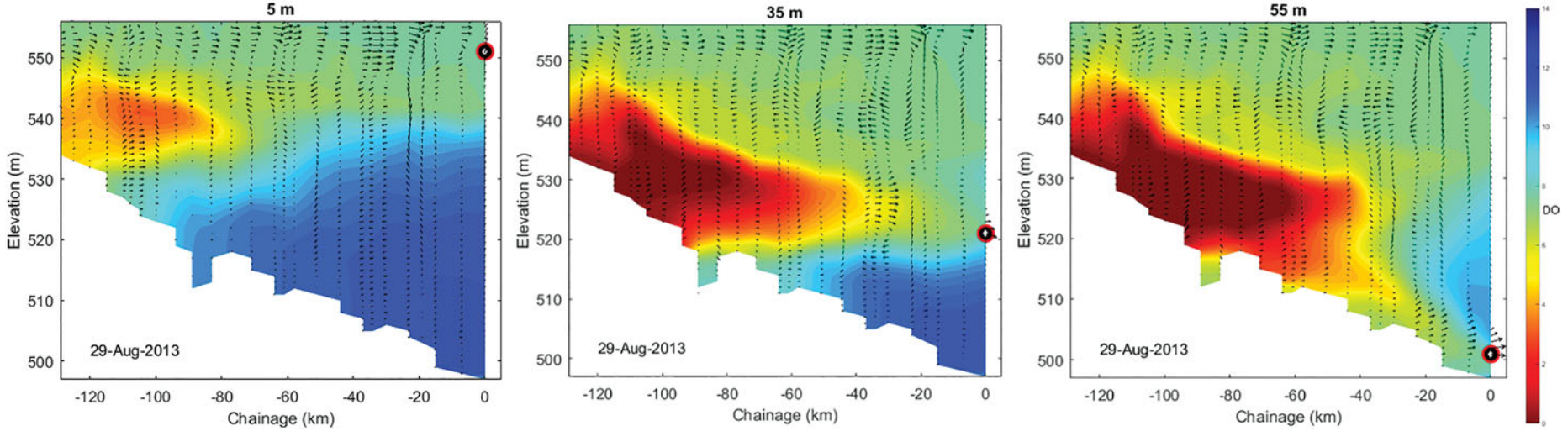

FIG. 13. August 29, 2013 DO profiles for 5, 35, and 55 m outflows during hypoxic conditions.

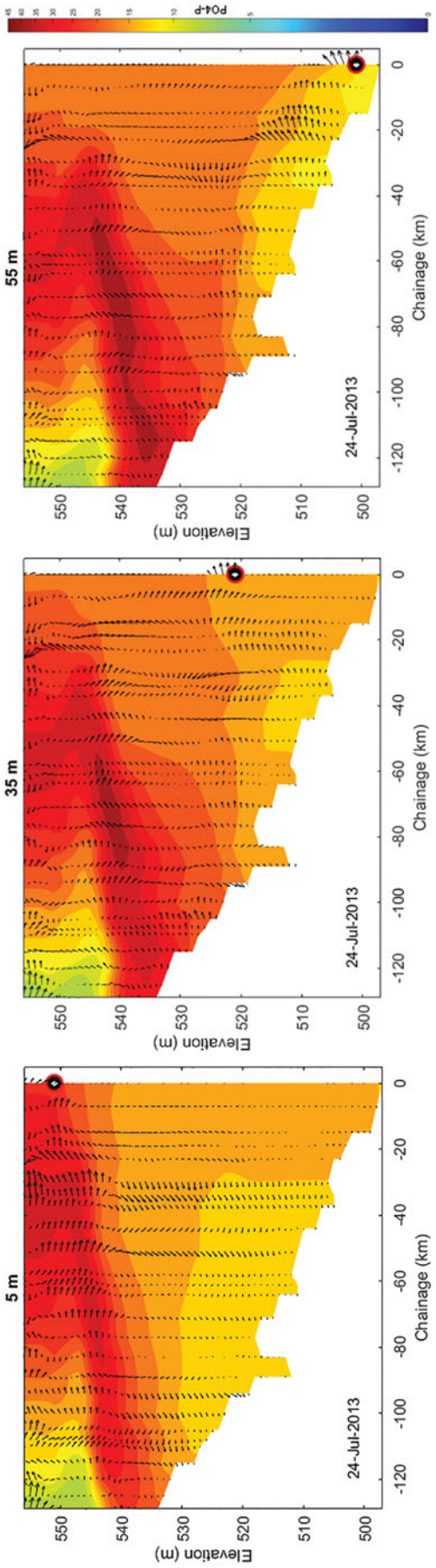

FIG. 14. July 24, 2013 PO_4^{3-} − P profiles for 5, 35, and 55 m outflows during hypoxic conditions.

Sadeghian *et al.*, 2017). Studies have shown that monthly allochthonous dissolved organic carbon (DOC) load is the main driver shaping reservoir hypolimnetic oxygen content and changes in oxygen may not follow temporal trends in TP or TN in the inflow (Marcé *et al.*, 2008). Although riverine and transition zones of Lake Diefenbaker can experience short periods of hypoxia, this typically happens once this region begins to stratify (Hudson and Vandergucht, 2015). This does not occur until late July in both years, well after the initial influx of turbid flows. Particularly large allochthonous organic inputs combined with short periods of stratification likely led to rapid DO depletion in 2013 (Hudson and Vandergucht, 2015).

The lag in decreased DO and increase in dissolved nutrients likely occurs because of nutrient desorption and DOC metabolism rates. Abstraction from the hypolimnion exasperates the low DO concentrations in the hypolimnion because the already warmer epilimnion causes the fine sediments to flow into layers of heavier density in the hypolimnion where the high DO demand is not replenished by reaeration. A study in a Polish reservoir (Dunalska *et al.*, 2007) found hypolimnetic withdrawal resulted in down welling of warm surface water, increasing hypolimnion temperature by 1.3°C that decreased strength of thermal stratification and increased phytoplankton primary production and biomass in the metalimnion. Conversely, they found that deep withdrawals reduced phytoplankton biomass in the hypolimnion (Dunalska *et al.*, 2014).

Here, in both years lower withdrawal elevations caused greater areas of low DO (Fig. 3) to spread within the reservoir. This was of particular concern in 2013 when an anoxic region formed mid-water column in the upstream half of the reservoir and lower elevations caused it to spread and cover a greater region of the reservoir. Transition zones of reservoirs often experience low DO during prolonged periods of stratification and reduced velocity results in deposition of finer materials and associated nutrients (Cole and Hannan, 1990; Kalff, 2002) (note the high concentrations of TP, PO_4^{3-}-P, TN, and NO_3^--N along the bottom, particularly in 2011). Greater June discharge in 2013 likely contributed to the influx of lower DO water into the reservoir along the surface and prolonged mixing of the water column into July. This routing of the surface water may also reduce surface warming causing lower surface temperatures than 2011 and pushing water with higher nutrient concentrations into the reservoir along the surface and mid-water column rather than only along the bottom.

Through July, surface velocities decreased substantially as spillway diversions decreased and high TP (Fig. 4) and water with low DO concentrations begin to move along the bottom of the reservoir rather than be routed along the surface. This is likely because of sediment beginning to settle along the bottom as decreased flow velocities decrease transport capacity. Through July 2011, higher TP and PO_4^{3-}-P concentrations move along the bottom of the reservoir and in 2013 higher concentrations move along the top of the reservoir. Greater June discharge in 2013 likely contributed to the influx of higher concentrations into the reservoir along the surface and delayed settling and/or mixing of nutrients in the water column. In both 2011 and 2013, summer water temperature, DO, and P concentrations (both TP and PO_4^{3-}-P) within the reservoir would be better controlled using shallow

withdrawal elevations. In 2011, there is little difference between outflow concentrations for different outflow scenarios; however, in 2013 this comes with a tradeoff of decreased DO and increased P and N transport downstream.

Under flood conditions, shallower withdrawal elevations would be advantageous for removing more limiting P from the water column and reducing epilimnion temperatures (particularly during peak flow periods) to reduce risks of harmful algal blooms. Temperatures above 25°C favor the growth of cyanobacteria (Paerl and Huisman, 2009) and shallow withdrawals during high flow events reduce temperatures and may also facilitate washout of harmful algal species that proliferate during the warmest periods (Roelke *et al.*, 2010). Similar to TP and PO_4^{3-}-P, water with high TN (Fig. 6) and NO_3^--N (Fig. 7) concentrations in 2011 is pulled deeper into the reservoir for low elevation outflows without changing outflow concentrations. However, in 2013, low elevations pull higher concentration water deeper but outflow concentrations decrease for both TN and NO_3^--N. Streamflow with greater concentrations of both TN and NO_3^--N enter the reservoir in 2013, again likely because of greater discharge in this year.

In 2013 (Figs. 12 and 13), DO levels decrease more than in 2011 (Fig. 9) with anoxic regions beginning to form in the upper half of the water column mid-July for the 500–540 masl scenarios. The regions of anoxia increase through July (Fig. 10) and an anoxic region was also formed for the 550 masl scenario (which declines by July 28). The anoxic regions remain in the upper riverine half of the reservoir. This agrees with previous studies that identified short periods of hypoxia in the riverine and transition zones of Lake Diefenbaker (Hudson and Vandergucht, 2015). In 2011, overall greater reservoir NO_3^--N concentrations occur through mid-August, before the period of lowest DO. However, regions of high PO_4^{3-}-P (Fig. 11) increase through July and August along the bottom in the hypoxic region. In 2013, TN and NO_3^--N concentrations peak near the surface at the end of June through the beginning of July, whereas overall reservoir NO_3^--N concentrations increase through July as anoxic regions grow. Regions of highest PO_4^{3-}-P (Fig. 14) concentrations coincide with July anoxic regions (Fig. 12). Hudson and Vandergucht (2015) suggested that this rapid DO depletion is likely caused by large allochthonous organic inputs during peak flows combined with short periods of stratification.

Through August, variable concentration patterns are similar to those in July, with 540 masl generally resulting in the best balance in reservoir and outflow temperatures and variable concentrations. Shallower withdrawal elevations seem to result in the most favorable reservoir and outflow variable concentrations during the summer stratification period. As mentioned previously, the portion of spillway outflow may contribute to this behavior by routing inflowing high concentration water across the surface and downstream more rapidly. The 540 and 530 masl elevations tend to be the optimal scenarios for balancing reservoir and outflow concentrations in summer.

There is little difference in both water temperature (Fig. A11 in Supplementary Appendix) and DO concentrations (Fig. A12 in Supplementary Appendix) between 2011 and 2013 and in both years shallower outflow scenarios tend to have more desirable concentrations/temperatures at both outflow and within the reservoir. The 530–540 masl outflows generally provide optimal concentrations for both DO and temperature. Lower elevation outflows maintain higher TP and PO_4^{3-}-P concentrations within the reservoir in both years (Figs. A13 and A14 in Supplementary Appendix). The same pattern is observed for TN and NO_3^--N (Figs. A15 and A16 in Supplementary Appendix). Here is little difference between both scenarios and years for NH_4^+-N (Fig. A17 in Supplementary Appendix). The largest fall spillway Q occurs in early October 2011 (Fig. A1 in Supplementary Appendix), although it appears to have little effect on the nutrient concentration distribution as vertical mixing has already begun.

There may be scenarios where there are tradeoffs between influencing phosphorus or nitrogen concentrations within the reservoir and at outflows, making identification of the optimal withdrawal elevation a challenge as outcomes can vary between years and from week to week in a given year. During spring turnover there is a slight tradeoff situation occurring. Optimal outflows to reduce NO_3^--N are the mid-depth 510–530 masl scenarios; however, optimal outflows for PO_4^{3-}-P reduction are 500 and 540 masl outflows. Despite this conflict, it makes sense to reduce the limiting nutrient P rather than N (Dubourg *et al.*, 2015). Therefore, 540 masl is likely the best elevation for reducing reservoir nutrient concentrations. During summer stratification and fall turnover 530–550 masl outflow scenarios are optimal for both P and N.

In addition to changes in variable concentrations and distribution, withdrawal elevation seems to influence volume of the epilimnion and hypolimnion and sediment distribution. Similarly, Zouabi-Aloui *et al.* (2015) also found that withdrawal depths had an influence on metalimnion thickness that influences strength of stratification, vertical transfer of heat, and DO. The abstractions from the lower elevations in Lake Diefenbaker are not only lowering the metalimnion but also contracting the volume of the hypolimnion. For every 10 m drop in the metalimnion, the hypolimnion volume is reduced by approximately half, $550\,m = (5{,}400 \times 10^6\ m^3)$, $540\,m = (2{,}700 \times 10^6\ m^3)$, $530\,m = (1{,}200 \times 10^6\ m^3)$, $520\,m = (500 \times 10^6\ m^3)$. Wind-induced flows along the surface are countered by reverse flows in the hypolimnion that are now concentrated with higher flows because of the smaller flow cross-section of the hypolimnion. Geomorphology also plays a role, in which flow velocities are increased even more where the lake bottom is narrower and more incised. In addition to the layering into deeper waters, the higher flows in the hypolimnion can draw more of the inflowing fine sediment along the lake bottom instead of transporting and diluting the sediment throughout the epilimnion when the abstraction is from the top layers. This is transferring the DO demand to the hypolimnion exacerbated by the lack of oxygen replenishment from reaeration and phytoplankton growth.

The model can now be used to explore other scenarios, particularly if there are shifts in reservoir management and operation strategies. Such shifts may include maintaining temperature coherence between the outflow river reach and the inflowing river to potentially improve diversity and habitat for animal species in the downstream river [e.g., macroinvertebrates—see Carr *et al.* (2019)]. In addition, the model can also be used to determine optimum abstraction levels to fulfill nutrient concentration thresholds in the downstream river reach for downstream water uses (e.g., water treatment plant at Saskatoon).

A limitation in this study is the lack of landscape interactions under climate change in the model. This may be

particularly important in the future as we enter a time of increased climate uncertainty and can be addressed using the approaches implemented by Nielsen *et al.* (2014) and Bucak *et al.* (2018). Optimum water quality levels in the reservoir can be reached by improving water releases management.

Model uncertainties

As with all models and studies of natural systems, there are different sources of uncertainty in this study. Data sparsity, both in terms of available measured variables and small spatial and temporal coverage, limited the ability to sufficiently calibrate all variables and include some important processes in simulations. For example, the model had very little data for phosphorous calibration and there are very few equations for the phosphorous mass balance. Therefore, using PO_4^{3-}-P (Fig. 6) as a proxy for soluble, bioavailable phosphorus, it appears that $\sim$50% of P entering the reservoir in May 2011 is in soluble form (7–20 μg/L) compared with particulate ($\sim$30–40 μg/L concentrations of total P) according to model output. This is an overestimation of TP as PO_4^{3-}-P tends to be in the 10–30% range in Diefenbaker reservoir (Abirhire *et al.*, 2015) and differs from Johansson *et al.* (2013) that found that 78.1–94.2% of external tributary TP loads to Lake Diefenbaker were particulate P. Despite these discrepancies, the model provides an accurate representation of how phosphorus is distributed within the reservoir regardless of higher than expected PO_4^{3-}-P concentrations.

There are also general uncertainties in the model structure preventing some processes from being included in the simulations. There were not enough data (*in situ* P release rates, Fe:P ratios, sulfate concentrations, ammonia release rates, etc.) to determine sediment nutrient remobilization; therefore, general assumptions about mobilization were made based on DO concentration. This was deemed appropriate as internal P loading is not considered a significant source of P to the reservoir in stratified regions such as at the dam outflow despite known P release from Lake Diefenbaker sediments year round (North *et al.*, 2015; Doig *et al.*, 2017).

Settling rates of suspended solids and algae were kept constant throughout the reservoir, although this is not representative. The reservoir is very large with complex geometry and bathymetry and a longitudinal shift from fluvial to lacustrine characteristics (variable velocities, depths, sedimentation, and erosion) (Sadeghian *et al.*, 2015). The upstream fluvial region is expected to have greater sedimentation rates than downstream because the majority of suspended particles in the lacustrine zone would be fine with low settling rates. An average settling rate was used throughout the lake as spatial and temporal changes in partitioning of particle size were not known. A Pareto optimum approach was applied to calibrate a general settling rate and the rate and critical stress for sediment resuspension. This is an optimization approach where two or more objective functions end up being slightly inaccurate to get a reasonable value overall, essentially identifying an acceptable compromise.

Conclusions

A 2D hydrodynamic CE-QUAL-W2 model has been implemented to simulate water withdrawal scenarios in a large multipurpose reservoir. The model is an effective tool for improving understanding of withdrawal elevation impacts on physical, chemical, and nutrient dynamics within Lake Diefenbaker. The main conclusions of this research are as follows:

- Deep abstractions draw down the metalimnion to increase the volume of the epilimnion and decrease the volume of the hypolimnion. Thermocline depth has been found to generally coincide with outlet depth. This increases the heat flux to the lake making the entire water body generally warmer and increasing density gradients. The metalimnion becomes thicker, with decreased temperature difference between the epilimnion and hypolimnion, but with a greater density gradient accentuating its behavior as a barrier between the epilimnion and hypolimnion.
- Deep abstractions also store more heat longer into the autumn season delaying turnover and winter inverse stratification. In the spring, deeper withdrawals generally increase downwelling of warmer surface waters leading to weaker summer stratification. With deep abstractions, the resulting smaller, more confined hypolimnion exhibits faster flow velocities along the lake bottom that draws in more of the inflowing sediment and associated nutrients into the hypolimnion, which was particularly apparent during summer stratification.
- The concentration of sediment along the bottom of the lake represents a strong DO deficit when the sediment material is decomposed. In general, deep abstractions draw more oxygen-rich surface water from the epilimnion into deeper layers. Although this usually results in shortened periods of anaerobic conditions near the bottom and diminished spatial extent of oxygen deficiency, it can have little effect on aerobic conditions.
- In general, during high flows when the spillway is in operation, water with high nutrient concentrations and low DO are routed along the surface in the region of highest flow velocities and water column mixing is delayed. This effect is only observed during summer stratification and not during turnover periods.
- P (TP and PO_4^{3-}-P) and NH_4^+-N concentrations within the reservoir would be better controlled using shallow withdrawal elevations. This comes with a tradeoff of increased P and N transport downstream. Under flood conditions, shallower withdrawal elevations would be advantageous for removing more limiting P from the water column and reducing epilimnion temperatures (particularly during peak flow periods) that may reduce risks of harmful algal blooms. Anoxia occur in the mid and bottom water depths through August peaking mid-September and lasting through the start of October. Greatest overall reservoir NO_3^--N and PO_4^{3-}-P concentrations coincide with hypoxic regions in both years.

Data Availability

All relevant data presented in this article are available in the online Federated Research Data Repository at https://www.frdr.ca/repo/handle/doi:10.20383/101.0134. Videos for the summer stratification period for the following years and time intervals: February 2011—0:20–0:50, 2012—2:22–2:52, 2013—4:23–4:54 can be seen at https://dx.doi.org/10.20383/101.0134.

Funding Information

Funding was provided by the University of Saskatchewan's Global Water Futures program.

Supplementary Material

Supplementary Appendix

References

Abirhire, O., North, R.L., Hunter, K., Vandergucht, D.M., Sereda, J., and Hudson, J.J. (2015). Environmental factors influencing phytoplankton communities in Lake Diefenbaker, Saskatchewan, Canada. *J. Great Lakes Res.* 41, 118.

Ashmore, P., and Day, T. (1988). Spatial and temporal patterns of suspended-sediment yield in the Saskatchewan River basin. *Can. J. Earth Sci.* 25, 1450.

Bucak, T., Trolle, D., Tavşanoğlu, Ü.N., Çakıroğlu, A.İ., Özen, A., Jeppesen, E., and Beklioğlu, M. (2018). Modeling the effects of climatic and land use changes on phytoplankton and water quality of the largest Turkish freshwater lake: Lake Beyşehir. *Sci. Total Environ*. 621, 802.

Çalişkan, A., and Elçi, S. (2009). Effects of selective withdrawal on hydrodynamics of a stratified reservoir. *Water Resour. Manage.* 23, 1257.

Carr, M., Li, L., Sadeghian, A., Phillips, I., and Lindenschmidt, K.-E. (2019). Modelling the possible impacts of climate change on the thermal regime and macroinvertebrate community of a regulated prairie river. *Ecohydrology* e2102.

Casamitjana, X., Serra, T., Colomer, J., Baseraba, C., and Pérez-Losada J. (2003). Effects of the water withdrawal in the stratification patterns of a reservoir. *Hydrobiologia.* 504, 21.

Cole, T.M., and Hannan, H.H. (1990). Ch. 4 Dissolved oxygen dynamics. In: K.W. Thornton, B.L. Kimmel, F.E. Payne, Eds., *Reservoir Limnology: Ecological Perspectives.* New York: Wiley.

Cole, T.M., and Wells, S.A. (2008). *User's Guide for CE-QUAL-W2: A Two-Dimensional, Laterally Averaged, Hydrodynamic and Water Quality Model, Version 3.5. Draft File Report 20314-1000.* Washington, DC: US Army Corps of Eng.

Doig, L.E., North, R.L., Hudson, J.J., Hewlett, C., Lindenschmidt, K.-E., and Liber, K. (2017). Phosphorus release from sediments in a river-valley reservoir in the northern Great Plains of North America. *Hydrobiologia* 787, 323.

Dubourg, P., North, R.L., Hunter, K., Vandergucht, D.M., Abirhire, O., Silsbe, G.M., Guildford, S.J., and Hudson, J.J. (2015). Light and nutrient co-limitation of phytoplankton communities in a large reservoir: Lake Diefenbaker, Saskatchewan, Canada. *J. Great Lakes Res.* 41, 129.

Dunalska, J.A., Staer, P.A., Jaworska, B., Górniak, D., and Gomułka, P. (2014). Ecosystem metabolism in a lake restored by hypolimnetic withdrawal. *Ecol Eng.* 73, 616.

Dunalska, J.A., Wiśniewski, G., and Mientki, C. (2007). Assessment of multi-year (1956–2003) hypolimnetic withdrawal from Lake Kortowski, Poland. *Lake Res. Manage.* 23, 377.

Fjeldstad, H.P., Uglem, I., Diserud, O.H., Fiske, P., Forseth, T., Kvingedal, E., Hvidsten, N.A., Okland, F., and Jarnegren, J. (2012). A concept for improving Atlantic salmon *Salmo salar* smolt migration past hydro power intakes. *J. Fish. Biol.* 81, 642.

Gelda, Rakesh K., and Steven, W. Effler. (2007). Simulation of operations and water quality performance of reservoir multilevel intake configurations. *J Water Resour Plann Manage.* 133.1, 78.

Huang, Z., and Wang, L. (2018). Yangtze dams increasingly threaten the survival of the Chinese sturgeon. *Curr. Biol.* 28, 3640.

Hudson, J.J., and Vandergucht, D.M. (2015). Spatial and temporal patterns in physical properties and dissolved oxygen in Lake Diefenbaker, a large reservoir on the Canadian Prairies. *J. Great Lakes Res.* 41, 22.

Johansson, J., Vandergucht, D., and Hudson, J. (2013). *Lake Diefenbaker Water Quality Sampling Progress Report (April 2012–March 2013).* Saskatoon: Saskatchewan Water Security Agency.

Kalff, J. (2002). *Limnology: Inland Water Ecosystems*. Upper Saddle River, NJ: Prentice Hall.

Ma, S., Kassinos, S.C., Fatta Kassinos, D., and Akylas, E. (2008). Effects of selective water withdrawal schemes on thermal stratification in Kouris Dam in Cyprus. *Lakes Reservoirs Res. Manage*. 13, 51.

Marcé, R., Moreno-Ostos, López, P., and Armengol, J. (2008). The roll of allochthonous inputs of dissolved organic carbon on the hypolimnetic oxygen content of reservoirs. *Ecosystems* 11, 1035.

McKinley, S., Van Der Kraak, G., and Power, G. (1998). Seasonal migrations and reproductive patterns in the lake sturgeon, *Acipenser fulvescens*, in the vicinity of hydroelectric stations in northern Ontario. *Environ. Biol. Fish*. 51, 245.

Morales-Marín, L.A., Wheater, H.S., and Lindenschmidt, K.E. (2017). Assessment of nutrient loadings of a large multipurpose prairie reservoir. *J. Hydrol.* 550, 166.

Nguyen, T.H., Everaert, G., Boets, P., Forio, M.A.E., Bennetsen, E., Volk, M., Hoang, T.H.T., and Goethals, P.L.M. (2018). Modelling tools to analyze and assess the ecological impact of hydropower dams. *Water.* 10, 1.

Nielsen, A., Trolle, D., Bjerring, R., Søndergaard, M., Olesen, J.E., Janse, J.H., Mooij, W.M., and Jeppesen, E. (2014). Effects of climate and nutrient load on the water quality of shallow lakes assessed through ensemble runs by PCLake. *Ecol Appl.* 24, 1926.

North, R.L., Johansson, J., Vandergucht, D.M., Doig, L.E., Liber, K., Lindenschmidt, K.-E., Baulch, H., and Hudson, J.J. (2015). Evidence for internal phosphorus loading in a large prairie reservoir (Lake Diefenbaker, Saskatchewan). *J. Great Lakes Res*. 41, 91.

Nürnberg, G.K. (2009). Assessing internal phosphorus load—problems to be solved. *Lake Reservoir Manage.* 25, 419.

Paerl, H.W., and Huisman, J. (2009). Climate change: A catalyst for global expansion of harmful cyanobacterial blooms. *Environ. Microbiol. Rep*. 1, 27.

Park, Y., Cho, K.H., Kang, J.-H., Lee, S.W., and Kim, J.H. (2014). Developing a flow control strategy to reduce nutrient load in a reclaimed multi-reservoir system using a 2D hydrodynamic and water quality model. *Sci. Total Environ*. 466, 871.

Phillips, I.D., Pollock, M.S., Bowman, M.F., McMaster, D.G., and Chivers, D.P. (2015). Thermal alteration and macroinvertebrate response below a large Northern Great Plains Reservoir. *J. Great Lakes Res*. 41, 155.

Pomeroy, J., and Shook, K. (2012). *Review of Lake Diefenbaker operations, 2010–2011.* Available at: www.usask.ca/hydrology/papers/Pomeroy_Shook_2012.pdf (accessed October 11, 2019).

Rheinheimer, D.E., Null, S.E., and Lund, J.R. (2014). Optimizing selective withdrawal from reservoirs to manage downstream temperatures with climate warming. *J. Water Resour. Plann. Manage.* 141, 04014063.

Roelke, D.L., Gable, G.M., and Valenti, T.W. (2010). Hydraulic flushing as a *Prymnesium parvum* bloom terminating mechanism in a subtropical lake. *Harmful Algae*. 9, 323.

Saadatpour, M., Afshar, A., and Edinger, J.E. (2017). Meta-model assisted 2D hydrodynamic and thermal simulation model (CE-QUAL-W2) in deriving optimal reservoir operational strategy in selective withdrawal scheme. *Water Resour. Manage*. 31, 2729.

Sadeghian, A., Chapra, S.C., Hudson, J., Wheater, H., and Lindenschmidt, K.-E. (2018). Improving in-lake water quality modeling using variable chlorophyll a/algal biomass ratios. *Environ. Modell. Software* 101, 73.

Sadeghian, A., de Boer, D., Hudson, J.J., Wheater, H., and Lindenschmidt, K.-E. (2015). Lake Diefenbaker temperature model. *J. Great Lakes Res.* 41, 8.

Sadeghian, A., Hudson, J., Wheater, H., and Lindenschmidt, K.-E. (2017). Sediment plume model—a comparison between use of measured turbidity data and satellite images for model calibration. *Environ. Sci. Pollut. Res.* 24, 19583.

Weagle, K., and Crosley, B. (1989). *Mass loading of phosphorus to Lake Diefenbaker. Water Quality Branch Report No. WQ 121*. Saskatchewan Environment and Public Safety, Regina, Saskatchewan, Canada.

Weber, M., Rinke, K., Hipsey, M.R., and Boehrer, B. (2017). Optimizing withdrawal from drinking water reservoirs to reduce downstream temperature pollution and reservoir hypoxia. *J. Environ. Manage.* 197, 96.

WSA. (2012). State of Lake Diefenbaker. Water Security Agency. Saskatchewan Water Security Agency, Saskatoon. (accessed December 6, 2018). https://www.wsask.ca/Global/Lakes and Rivers/Dams and Reservoirs/Operating Plans/Developing an Operating Plan for Lake Diefenbaker/State of Lake Diefenbaker Report-October 19 2012.pdf

Zheng, T., Sun, S., Liu, H., Xia, Q., and Zong, Q. (2017). Optimal control of reservoir release temperature through selective withdrawal intake at hydropower dam. *Water Sci. Technol*. 17.1, 279.

Zouabi-Aloui, B., Adelana, S.M., and Gueddari, M. (2015). Effects of selective withdrawal on hydrodynamics and water quality of a thermally stratified reservoir in the southern side of the Mediterranean Sea: A simulation approach. *Environ. Monit. Assess*. 187, 292.